Mathematical Medicine and Biology Page 1 of 29
doi:10.1093/imammb/dqnxxx

Bifurcation analysis of a phage-bacteria interaction model with prophage induction

H. M. NDONGMO TEYTSA[2,3] B. TSANOU[1,2,3] S. BOWONG[3,4] J. M.-S. LUBUMA[1]

[1]*Department of Mathematics and Applied Mathematics, University of Pretoria, Pretoria 0002, South Africa*

[2] *Department of Mathematics and Computer Science, University of Dschang, P.O. Box 67 Dschang, Cameroon.*

[3]*IRD UMI 209 UMMISCO, University of Yaounde I, P.O. Box 337 Yaounde, Cameroon and LIRIMA-EPITAG Team Project, University of Yaounde I, P.O. Box 812 Yaounde, Cameroon*

[4]*Department of Mathematics and Computer Science, University of Douala, P.O. Box 24157, Cameroon*

[Received on]

A prey-predator model is used to investigate the interactions between phages and bacteria by considering the lytic and lysogenic life cycles of phages and the prophage induction. We provide answers to the following conflictual research questions: (1) what are conditions under which the presence of phages can purify a bacterial infected environment? (2) can the presence of phages triggers virulent bacterial outbreaks? We derive the basic offspring number $\mathscr{N}_0$ which serves as a threshold and the bifurcation parameter to study the dynamics and bifurcation of the system. The model exhibits three equilibria: An unstable environment-free equilibrium (EFE), a globally asymptotically stable (GAS) phage-free equilibrium (PFE) whenever $\mathscr{N}_0 < 1$, and a locally asymptotically stable (LAS) environment-persistent equilibrium (EPE) when $\mathscr{N}_0 > 1$. The Lyapunov-LaSalle techniques are used to prove the GAS of the PFE and estimate the EPE basin of attraction. Through the center manifold approximation, topological types of the PFE are precised. Existence of transcritical and Hopf bifurcations are established. Precisely, when $\mathscr{N}_0 > 1$, the EPE loses its stability and periodic solutions arise. Furthermore, increasing $\mathscr{N}_0$ can purify an environment where bacteriophages are introduced. Purposely, we prove that for large values of $\mathscr{N}_0$, the overall bacterial population asymptotically approaches zero, while the phage population sustains. Ecologically, our results show that for small values of $\mathscr{N}_0$, the existence of periodic solutions could explain the occurrence of repetitive bacteria-borne disease outbreaks, while large value of $\mathscr{N}_0$ clears bacteria from the environment. Numerical simulations support our theoretical results.

Keywords:
Bifurcation, stability, phage-bacteria, prophage induction, lytic life cycle, lysogenic life cycle.

1. Introduction

Phages or bacteriophages are actually viruses that infect bacteria. They are obligate intracellular parasites which rely on the bacteria hosts in order to replicate. Phages are an essential part of the aquatic biology because of their omnipresence in the aquatic ecosystem. They are closely linked to the bacterial population. Based on their survival life strategies, phages exhibit three different life cycles which are lytic, lysogenic and pseudo-lysogenic (see Bhandare & Sudhakar G (2005), Miller R. V., & Day M.(2008)). In the lytic life cycle, the phage injects the bacterium cell, multiplies and progeny phages burst from the cell killing the bacterium. In the lysogenic life cycle, the phage does not replicate but its

genome goes into a quiescent condition and is usually integrated into the host genome or alternatively it may be maintained as an extra chromosomal plasmid (see Bhandare & Sudhakar G. (2005), Miller R. V., & Day M. (2008)). The integrated phage genome is called a prophage while a bacterial host with a prophage is called a lysogen bacterium. The lysogenic life cycle allows the host cell to continue to survive and reproduce, the virus is reproduced in all of the cell's offsprings. In the pseudo lysogenic life cycle, the phage does not undergo lysogeny nor does it show lytic life cycle but it remains in a non active state. There are some phages which can enter either the lytic or lysogenic life cycle. Phages that replicate only via the lytic life cycle are known as virulent phages while those that replicate using both lytic and lysogenic life cycles are known as temperate phages.

In the lysogenic life cycle, upon detection of cell damage, such as UV radiation light or certain chemical, the prophage is extracted from the bacterial chromosome in a process called prophage induction (see Bhandare & Sudhakar G. (2005)). After induction, viral replication begins via the lytic life cycle.

The presence of phages in an environmental reservoir plays an essential role in the evolution of bacterial species. Thus, on the one hand, the interaction between phages and bacteria can contribute to trigger some environmental indirectly transmitted diseases by enabling the emergence of new clones of virulent pathogenic bacteria. For instance, Vibrio cholerae, the causative agent of cholera epidemics represents a paradigm for this process. In fact, the latter organism evolves from environmental non-pathogenic strains to highly pathogenic species by acquisition of virulent genes through the lysogenic life cycle in the phage-bacteria interactions (see Faruque M. & John J. (2012)). The major virulence factors of V. cholerae which are cholera toxin (CT) and toxin coregulated pilus (TCP) are encoded by a lysogenic phage (CTXϕ) and a pathogenicity island, respectively (see Faruque M. & John J. (2012)). Hence, the importance of incorporating the lysogenic life cycle in the models that describe the interactions between phages and bacteria in the environmental reservoir with the ultimate aim to explain the triggering of bacterial related disease outbreaks. On the other hand, the presence of phages in an environmental reservoir of bacteria can purify this environment by driving the population of bacteria to extinction. Therefore, two main research questions come into play: (1) What are conditions under which the presence of phages can purify a bacterial polluted environment? (2) Conversely, in which situations can the presence of phages triggers virulent pathogenic bacterial disease outbreaks?

Understanding the genetic and ecological factors which support the phage-bacteria interactions and the production of highly virulent pathogenic species is vital to develop preventive measures. In this struggle, Mathematical Biology/Ecology is an essential tool and provides insights into the co-evolution or extinction of bacteria and phages.

Many mathematical models have been published to study the marine phages infection and for the most recent works among others, we refer the reader to (Beretta E.& Y. Kuang (1998), Lui F., Cortez M.& Weitz J. (2013), Yu P., Nadeem A. & Wall L. M. (2017), Sukhita & Vidurupola W.(2018). Unlike the large number of models describing the lytic life cycle of phage-bacterium interaction, very little effort has been devoted to the lysogenic life cycle and prophage induction and the combination of both. In Yu P., Nadeem A. & Wall L. M. (2017), the authors proposed a model to study the impact of prophage on the equilibria and stability of phage and bacterium host. In their model, the lysogen bacteria population does not appear explicitly since they considered that the infected bacteria cannot reproduce. More Recently in Xueying W. &Jin W. (2017), the deterministic and stochastic models for the within-host dynamics of cholera with a focus on the interaction between phages and vibrio cholerae in the human host was proposed. Contrary to Yu P., Nadeem A. & Wall L. M.(2017), an equation for the lysogen bacteria population appeared explicitly in Xueying W. & Jin W. (2017), yet the prophage induction was still neglected. To fill the above mentioned gaps, we extend the deterministic models of Yu P., Nadeem

A. & Wall L. M. (2017), Xueying W. & Jin W. (2017) by considering both the lytic and lysogenic life cycles of phages and prophage induction altogether. More precisely, since the genetic material of phages (called prophage) can be transmitted to bacterial daughter cells at each subsequent cell division, we propose a mathematical model that additionally takes into account the fact that in the lysogenic life cycle, the virus reproduces in all the cell's offsprings. The propounded model is a predator-prey like system with Holling type functional response. We use it to provide possible responses to the above-mentioned research questions, which are rooted on the range of the basic offspring number of phages. The basic offspring number $\mathscr{N}_0$ is computed and used to examine the global dynamics and perform an in-depth bifurcation analysis of the system and the three equilibria exhibited are topologically classified as follows: An unstable environment-free equilibrium (EFE), a globally stable phage-free equilibrium (PFE) whenever $\mathscr{N}_0 < 1$, and a unique locally stable environment-persistent (EPE) equilibrium which exits when $\mathscr{N}_0 > 1$. We use a suitable Lyapunov function to estimate the basin of attraction of EPE. The model undergoes a trans-critical forward bifurcation at $\mathscr{N}_0 = 1$ and a Hopf bifurcation around the EPE. Precisely, we show that when $\mathscr{N}_0 > 1$, there is a critical value $\mathscr{N}_0^c$ such that for $\mathscr{N}_0 \geqslant \mathscr{N}_0^c$, the EPE loses its stability through the appearance of a Hopf bifurcation, given rise to periodic solutions.

The rest of the paper is organized as follows: in Section 2, the mathematical model is formulated. We derive its basic properties, compute and perform the sensitivity analysis of the basic offspring number $\mathscr{N}_0$ in Section 3. The main Section 4 is devoted to the existence of equilibria, their global stability and the bifurcation analysis of the model based on the range of $\mathscr{N}_0$. Section 5 deals with the global sensitivity analysis of the model's variables. The last Section 6 concludes the paper and provides some discussions on the limitations of this work and for future investigations.

2. Model derivation context

To place our model derivation in a specific context, we provide the main modeling hypotheses.
(H1) Since in the pseudo lysogenic, the phages are inactive, we neglect it and focus only on the lytic and lysogenic life cycles.
(H2) We assume that there are enough bacteria in the aquatic environment for the phage-bacteria interactions to last for sufficiently longer time.
(H3) We consider the logistic growth for the bacteria species and the Holling-type II functional response for the interactions between phages and bacteria. This is justified by the fact many bacteria are free-living pathogens capable of self multiplication in their biotope.
(H4) We suppose that in the presence of phages (or viruses) population P, the population of bacteria splits into three different classes: (i) The susceptible bacteria are B (not yet attacked by the phages). (ii) The lysogen bacteria population V (those bacteria infected by lysogenic phages), and recall that the during the lysogenic life cycle, instead of killing the host, the phage genome integrates into the bacterial chromosome and becomes part of the host. (iii) The population of infected bacteria Z (those bacteria infected by lytic phages), whose equation decouples from the system as we shall see shortly.

Following assumption (H3) our model introduces a threshold for the susceptible bacteria known as carrying capacity K, so that initially, the population grows exponentially and later stabilizes at a constant level $K > 0$. Susceptible bacteria acquire infection at rate $\beta B/(B+H)$ known as Holling-type II functional response. In the latter, β stands for the contact between the susceptible bacterial cells and phages/viruses. The bacterial mortality rate in the reservoir is μ. The dynamics of B is therefore modeled by the following equation

$$\frac{dB}{dt} = rB\left(1 - \frac{B}{K}\right) - \beta\frac{BP}{B+H} - \mu B. \tag{2.1}$$

Symbols	Biological definitions	Baseline value	Range	Source
B	Density of susceptible bacteria			
V	Density of lysogen bacteria			
P	Density of free phage population			
Z	Density of infected bacteria			
r	Intrinsic bacteria growth rate	0.8	$0.3-14.3$	(see Jensen A. (2006))
K	Bacteria carrying capacity	10^5	10^5-10^7	(see Kong J.(2014))
H	Half-saturation bacteria density	10^6	10^6-10^8	(see Kong J.(2014))
β	Phage-bacterium contact rate	0.15	$0.1-0.9$	(see Jensen A. (2006))
α	Prophage induction rate	0.4	$0.001-0.99$	assumed
ϕ	Cell division size	80	$10-100$	assumed.
π	Fraction of lysed bacteria	0.7	$0.5-1$	assumed
θ	Burst size	100	$80-100$	(see Jensen A. (2006))
μ	Bacteria death rate	0.15	$0.4-0.99$	assumed.
δ	Phages death rate	0.5	$0.5-7.9$	(see Jensen A. (2006))
γ	Bacteria death rate due to lysis	1	$0.1-1$	assumed

Table 1. Variables and parameters for model (2.4).

For Eq. (2.1) to be ecologically meaningful, and the whole interaction system to be mathematically tractable, we assume that $r > \mu$. Otherwise, the bacteria population B will collapse in finite time.

Phages can undergo a lytic or a lysogenic life cycle, whereas few are capable of carrying out both. We denote by π the fraction of infected cells that burst and produce new phages, while $(1-\pi)$ is the fraction of lysogen bacteria. The lysogenic life cycle allows the bacterial host cell to continue to survive and reproduce, the phage is reproduced in all of the cell's offsprings and we denote the bacterial cell multiplication size by ϕ. In the course of this division, the effect of UV radiations or the presence of certain chemicals can lead to the release of prophage causing proliferation of new phages through the prophage induction. Therefore, we denote by α the rate of lysogen bacteria who switch from a the lysogenic life cycle to the lytic life cycle. So the dynamic of lysogen bacteria is:

$$\frac{dV}{dt} = \phi(1-\pi)\frac{\beta BP}{B+H} - (\alpha+\mu)V. \tag{2.2}$$

In the lytic life cycle, bacteria cells burst (lysed) and destroyed after immediate replication of the new phages; we denote by θ the burst size of the bacteria. Hence, the dynamic of phages is modeled by the following equation.

$$\frac{dP}{dt} = \theta\pi\beta\frac{BP}{B+H} + \theta\alpha V - \delta P. \tag{2.3}$$

The Figure 1 describes the interactions between lytic phages, lysogenic phages, bacteria and the prophage induction event. The parameters and variables of the model (2.4) are summarized in Table 1. Based on the above mentioned formulation and assumptions, we schematically simplify the phage bacteria interactions in Figure 2 from which we derive the following system of non-linear differential equations.

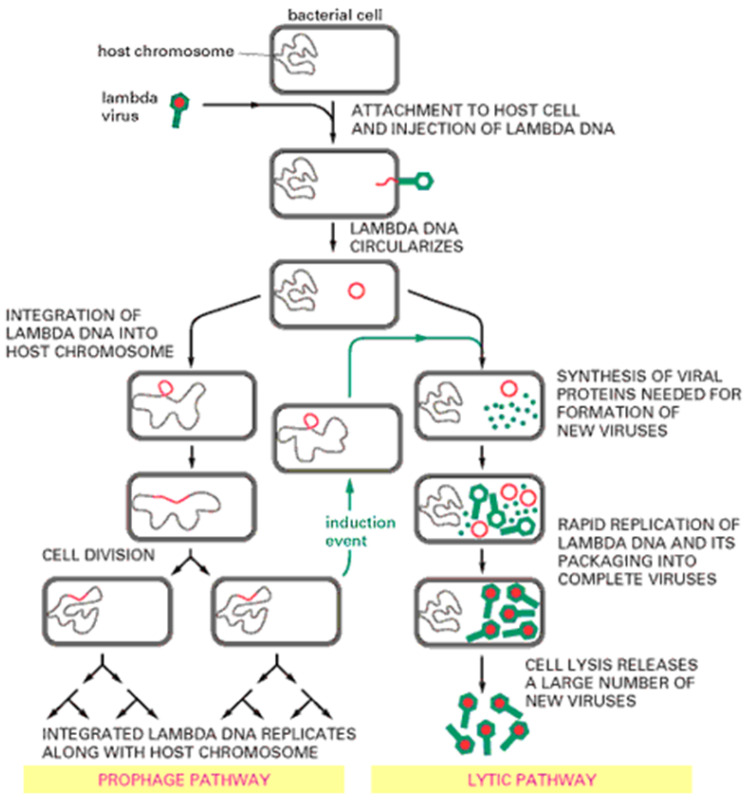

FIG. 1. Phage-Bacteria interactions and prophage induction process.

$$\begin{cases} \dfrac{dB}{dt} = rB\left(1-\dfrac{B}{K}\right) - \beta\dfrac{BP}{B+H} - \mu B, \\ \dfrac{dV}{dt} = \phi(1-\pi)\beta\dfrac{BP}{B+H} - (\alpha+\mu)V, \\ \dfrac{dP}{dt} = \theta\pi\beta\dfrac{BP}{B+H} + \theta\alpha V - \delta P. \end{cases} \tag{2.4}$$

It should be noted that the equation for the dynamics of the infected bacteria Z, which actually decouples from (2.4) is given by:

$$\frac{dZ}{dt} = \pi\beta\frac{BP}{B+H} + \alpha V - (\mu+\gamma)Z. \tag{2.5}$$

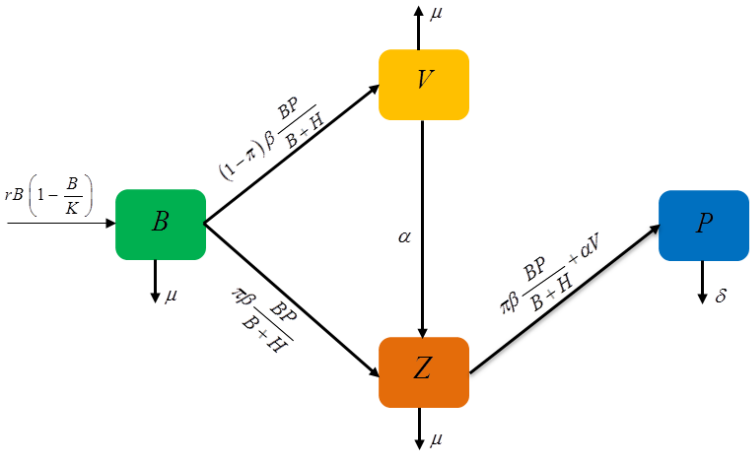

FIG. 2. Schematic representation of the phage-bacteria interactions.

3. Basic mathematical properties and basic offspring number

3.1 *Existence, uniqueness and positivity of solutions*

For the model (2.4) to be ecologically meaningful, it is important to prove that all the state variables are non-negative for all time t. In the other words, the solution of the model (2.4) with positive initial data should remain positive for all $t \geqslant 0$. Setting

$$N(t) = \phi B(t) + V(t),\ \zeta = min(\mu, \delta),\ \text{and}\ P_{max} = (\theta\pi rK + \theta\alpha\phi rK)/(4\mu\zeta),$$

we summarize these basic properties in the following result.

THEOREM 3.1 The system (2.4) is a dynamical system in

$$\Omega = \left\{ (B,V,P) \in \mathbb{R}^3_+,\ N(t) \leqslant \frac{\phi rK}{4\mu},\ P(t) \leqslant P_{max} \right\}.$$

Proof : From the first equation of (2.4), one has

$$\frac{dB}{B} = \psi(B,P), \quad \text{where} \quad \psi(B,P) = \left\{ r - \mu - \frac{rB}{K} - \frac{\beta P}{B+H} \right\}.$$

The integration of the previous equation from 0 to t gives,

$$B(t) = B(0)e^{\int_0^t \psi(B,P)} > 0 \quad \forall t > 0.$$

Considering the fact that $B(t) > 0$, and discarding for now the equation for the susceptible bacteria $B(t)$, the remaining sub-system for the compartments V and P takes the form

$$\dot{x} = Mx, \tag{3.1}$$

where, $x = (V,P)$, and $M = \begin{pmatrix} -(\mu+\alpha) & \dfrac{\phi(1-\pi)\beta B}{B+H} \\ \theta\alpha & \theta\pi\beta\dfrac{B}{B+H} - \delta \end{pmatrix}$.

M is a Metzler matrix and the system (3.1) is cooperative, so if $V(0)$, $P(0) \geqslant 0$, then $V(t)$, $P(t) \geqslant 0$ $\forall t > 0$. Moreover,

$$\begin{aligned} \dot{N} = \phi\frac{dB}{dt} + \frac{dV}{dt} &\leqslant \phi rB\left(1-\frac{B}{K}\right) - \mu(\phi B+V) + \phi(1-\pi)\beta\frac{BP}{B+H} - \phi\beta\frac{BP}{B+H} \\ &\leqslant \phi rB\left(1-\frac{B}{K}\right) - \mu(\phi B+V) \\ &= \phi rB\left(1-\frac{B}{K}\right) - \mu N. \end{aligned}$$

Knowing that

$$\max_{0\leqslant B\leqslant K}\left\{B\left(1-\frac{B}{K}\right)\right\} = \frac{K}{4},$$

we have,

$$\dot{N} \leqslant \phi r\frac{K}{4} - \mu N.$$

Using a Granwall lemma (see Lakshmikantham S. & Leela. M. (1989)), we show that

$$N(t) \leqslant N(0)e^{-\mu t} + \phi r\frac{K}{4\mu}(1-e^{-\mu t}).$$

Thus, if $N(0) \leqslant \phi rK/4\mu$, then $N(t) \leqslant \phi rK/4\mu$, for all $t \geqslant 0$.

Similarly, if we set $Y = \theta\pi B + P$, then

$$\begin{aligned} \dot{Y} &= \theta\pi rB\left(1-\frac{B}{K}\right) - \mu\pi\theta B + \theta\alpha V - \delta P \\ &\leqslant \frac{\theta\pi rK + \theta\alpha\phi rK}{4\mu} - \zeta Y. \end{aligned}$$

Another application of a Gronwall lemma gives $P(t) \leqslant P_{max}$ for all $t \geqslant 0$, if $P(0) \leqslant P_{max}$. Thus Ω is a positively invariant set under the flow of system (2.4). Hence it is sufficient to consider the dynamics of the model (2.4) in Ω. □

3.2 *Basic offspring number and its sensitivity analysis*

For notational simplicity, let's denotes $B_0 = K(r-\mu)/r$, so that the PFE of model (2.4) is $E_1 = (B_0, 0, 0)$. Note that the disease components in model (2.4) are V and P. The matrix for the new offsprings and that for the transition between compartments are respectively

$$F = \begin{pmatrix} 0 & \dfrac{\phi(1-\pi)\beta B_0}{B_0+H} \\ 0 & \dfrac{\theta\pi\beta B_0}{B_0+H} \end{pmatrix} \quad \text{and} \quad W = \begin{pmatrix} \alpha+\mu & 0 \\ -\theta\alpha & \delta \end{pmatrix}.$$

By the next generation matrix method (see Driessche P.V.D. & Wathmough J. (2002)), the basic offspring number is defined as the spectral radius of the next generation matrix FW^{-1} of the model (2.4) which is given by

$$FW^{-1} = \begin{pmatrix} \dfrac{\theta\alpha\phi(1-\pi)\beta B_0}{\delta(\mu+\alpha)(B_0+H)} & \dfrac{\phi(1-\pi)\beta B_0}{\delta(B_0+H)} \\ \dfrac{\theta}{\delta(\mu+\alpha)}\dfrac{\theta\pi\beta B_0}{B_0+H} & \dfrac{1}{\delta}\dfrac{\theta\pi\beta B_0}{B_0+H} \end{pmatrix}.$$

Since FW^{-1} is a rank 1 matrix, the basic offspring number of the model (2.4) (i.e. the spectral radius of FW^{-1}) is given by its trace as follows:

$$\mathcal{N}_0 = \rho(FW^{-1}) = \frac{\theta\pi\beta B_0}{\delta(B_0+H)} + \frac{\theta\alpha\phi(1-\pi)B_0}{\delta(\mu+\alpha)(B_0+H)}. \tag{3.2}$$

REMARK 3.1 Notice that, if one uses the full model (2.4)-(2.5) to compute the basic offspring number $\mathcal{N}_0$ following the approach in (Driessche P.V.D. & Wathmough J. (2002)), the variable Z should be added to the set of disease components. As expected, the expression for the basic offspring number $\mathcal{N}_0$ remains unchanged. This outcome shouldn't be surprising because the variable $Z(t)$ does not appear in the equations for $B(t), V(t)$ and $P(t)$, and therefore cannot influence their dynamics.

For the biological interpretation of the basic offspring number $\mathcal{N}_0$, pose

$$f(B) = \frac{\beta B}{B+H}, \quad \mathcal{N}_{0Z} = \frac{\theta\pi f(B_0)}{\delta}, \quad \mathcal{N}_{0V} = \frac{\theta\phi(1-\pi)f(B_0)}{\delta}\frac{\alpha}{\alpha+\mu}.$$

Thus, with these notations, $\mathcal{N}_0$ reads

$$\mathcal{N}_0 = \mathcal{N}_{0Z} + \mathcal{N}_{0V}. \tag{3.3}$$

Different terms in $\mathcal{N}_{0Z}$ and $\mathcal{N}_{0V}$ given by (3.3) can be interpreted as follows:
• $\theta\pi f(B_0)$ is the mean number of new phages released after burst of bacteria via the lytic life cycle.
• $\theta\phi(1-\pi)f(B_0)$ is the mean number of new phages produced through the prophage induction process.
• $\alpha/(\alpha+\mu)$ is the probability that a lysogen bacterium undergoes a lytic life cycle through the prophage induction process.
• $1/\delta$ is the average lifespan of phages.
Thus, $\mathcal{N}_{0Z}$ is the mean number of phage offsprings produced by a single phage, in the fully uninfected bacteria population via the lytic life cycle of the phage, whereas $\mathcal{N}_{0V}$ gives the mean number of phage offsprings generated through the prophage induction process, by a single phage introduced in the fully uninfected bacteria population. The sum $\mathcal{N}_0 = \mathcal{N}_{0Z} + \mathcal{N}_{0V}$ is therefore the mean number of phage offsprings generated by a single phage, either in the lytic or lysogenic life cycle, introduced into the fully uninfected population of bacteria.

The local sensitivity analysis is based on the normalized sensitivity index of $\mathcal{N}_0$. The normalized forward sensitivity index of a variable to a parameter is the number of the relative change in the variable to the relative change in the parameter. Since the basic offspring number is a differentiable function with respect to any of its parameters, the sensitivity indices are calculated using partial derivative of $\mathcal{N}_0$ (see Gjorgjieva J., Smith K., Chowell G., Sanchez F., Snyder D. & Castillo C. (2005)) and are displayed in Table 2 below.

Parameters	Sensitivity index	Value
r	$S_r^{\mathcal{N}_0}$	+0.0277
β	$S_\beta^{\mathcal{N}_0}$	$+1$
μ	$S_\mu^{\mathcal{N}_0}$	-0.5372
δ	$S_\delta^{\mathcal{N}_0}$	-1
α	$S_\alpha^{\mathcal{N}_0}$	$+0.5709$
K	$S_K^{\mathcal{N}_0}$	+0.9248
H	$S_H^{\mathcal{N}_0}$	-0.9248
θ	$S_\theta^{\mathcal{N}_0}$	+1
ϕ	$S_\phi^{\mathcal{N}_0}$	+0.9320

Table 2. Normalized sensitivity indexes of $\mathcal{N}_0$: The phage-bacteria contact rate β, the lysis burst size θ, the phage death rate δ, the bacteria cell division rate ϕ, in the decreasing order, the susceptible bacteria carrying capacity K, the half-saturation bacteria density H, are the most influential parameters on $\mathcal{N}_0$. Note that the baseline values in Table 1 should have been used here to compute the sensitivity indexes.

To this aim, denoting by ψ the generic parameter of system (2.4), we evaluate the normalized sensitivity index

$$S_\psi^{\mathcal{N}_0} = \frac{\psi}{\mathcal{N}_0}\frac{\partial \mathcal{N}_0}{\partial \psi}. \tag{3.4}$$

Mathematically, $S_\psi^{\mathcal{N}_0}$ indicates how sensitive $\mathcal{N}_0$ is to the change of parameter ψ. A positive (resp. negative) index indicates that an increase in the parameter value results in an increase (resp. decrease) in the $\mathcal{N}_0$ value.

It is worth noticeable that local sensitivity analysis only assesses the effects of individual parameters at particular point in parameter space, without considering the combined variability resulting from all input parameters simultaneously. To address the latter, we perform a global sensitivity analysis to obtain the model response to parameter variation within a wider range in parameter space. Following the approach Gjorgjieva J., Smith K., Chowell G., Sanchez F., Snyder D. & Castillo C. (2005) , PRCC between $\mathcal{N}_0$ and each parameter are derived. The results of the PRCCs of $\mathcal{N}_0$ are shown in Figure 3.

REMARK 3.2 From Table 2 and Figure 3, we observe that the parameters β, α, K, θ and ϕ have the most positive influence (by augmenting it) on $\mathcal{N}_0$, while have remarkable negative impact (by reducing it) on $\mathcal{N}_0$ are δ, H and μ. For instance, the increase of β, α, K, θ and ϕ, say by 10%, will increase $\mathcal{N}_0$ by 10%, 9.2%, 10% and 9.3%, respectively.

According to the Figure 3, $\mathcal{N}_0$ is highly sensitive to the bacteria cell division size ϕ. Since the prophage induction parameter α is central in this work, because ϕ and α are keys parameters characterizing the prophage induction, one may wish to assess their combined influence on the basic offspring $\mathcal{N}_0$, with the ultimate aim to control the growth of lysogen bacteria, which are thought to be responsible of severe disease outbreaks. This is investigated in Figure 4. More importantly, the matching of the local sensitivity analysis (see Table 2) and global sensitivity analysis (see Figure 3) of $\mathcal{N}_0$ demonstrates its robustness to the parameters variations.

Figure 4 precisely shows that, for a large value (say, $\phi = 90$) of the cell division size ϕ, $\mathcal{N}_0$ is always

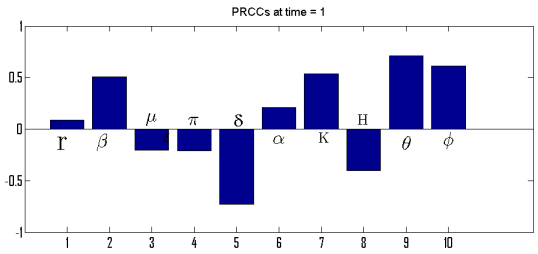

FIG. 3. PRCC$_s$ of $\mathcal{N}_0$: This global sensitivity analysis is consistent with the local sensitivity of $\mathcal{N}_0$, except that the bacteria burst size θ overcome the phage-bacteria contact rate β. However, as a whole the basic offspring number $\mathcal{N}_0$ is highly robust to its parameters variation.

greater than one, regardless the value of α. However, if the value of ϕ is halved (say, $\phi = 45$), then one should increase the value of α above 0.15 to bring $\mathcal{N}_0$ above one. This underscores the importance of prophage induction in controlling the bacteria population, since it is only when $\mathcal{N}_0 > 1$ that more phages are produced to destroy more bacteria.

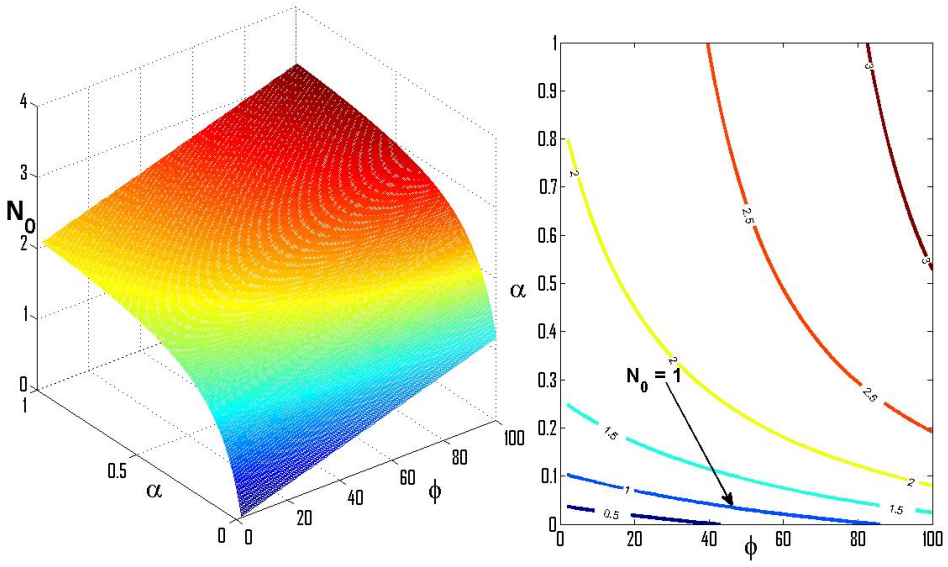

FIG. 4. Graph and Contour plots of $\mathcal{N}_0$ versus induction rate α and cell division size ϕ.

4. Equilibria and bifurcation analysis

4.1 *Existence of equilibria and trans-critical forward bifurcation at* $\mathscr{N}_0 = 1$

Clearly, if $P = 0$, then the model (2.4) admits two trivial equilibria: the EFE $E_0 = (0,0,0)$ and the PFE $E_1 = (B_0,0,0)$. The EPE $E^* = (B^*,V^*,P^*)$ of model (2.4) satisfies the system

$$\begin{cases} rB^*\left(1-\dfrac{B^*}{K}\right) - \beta\dfrac{B^*P^*}{B^*+H} - \mu B^* = 0, \\ \phi(1-\pi)\beta\dfrac{B^*P^*}{B^*+H} - (\alpha+\mu)V^* = 0, \\ \theta\pi\beta\dfrac{B^*P^*}{B^*+H} + \theta\alpha V^* - \delta P^* = 0. \end{cases} \tag{4.1}$$

From the second equation of (4.1), we have

$$V^* = \frac{\phi(1-\pi)\beta}{(\mu+\alpha)}\frac{B^*P^*}{B^*+H}. \tag{4.2}$$

The substitution of the expression for V^* into the third equation of (4.1) yields

$$\left(\theta\pi\beta + \frac{\theta\alpha\phi(1-\pi)\beta}{(\mu+\alpha)}\right)\frac{B^*P^*}{B^*+H} - \delta P^* = 0.$$

Since we are looking for the positive equilibria, then $P^* > 0$, we are left with the equation

$$\left(\theta\pi\beta + \frac{\theta\alpha\phi(1-\pi)\beta}{(\mu+\alpha)}\right)\frac{B^*}{B^*+H} - \delta = 0. \tag{4.3}$$

After some computations we have the following expression of B^*

$$B^* = \frac{HB_0}{B_0(\mathscr{N}_0-1)+H\mathscr{N}_0}. \tag{4.4}$$

From the first equation of (4.1),

$$B^*\left(r-\mu-\frac{rB^*}{K}\right) = \beta\frac{B^*P^*}{B^*+H}.$$

That is

$$\frac{r}{K}(B_0-B^*) = \beta\frac{P^*}{B^*+H}.$$

From equation (4.4), we have

$$B_0 - B^* = \frac{B_0(B_0+H)(\mathscr{N}_0-1)}{B_0(\mathscr{N}_0-1)+H\mathscr{N}_0}. \tag{4.5}$$

We note that, since the basic offspring number $\mathscr{N}_0 > 1$, it is clear from (4.5) that $B^* < B_0$, and

$$P^* = \frac{r}{\beta K}(B_0-B^*)(B^*+H).$$

Using the expression of B^* given by (4.4), and the expression (4.5) it is easy to obtain the formula for P^* below.

$$P^* = \frac{rH}{\beta K}\frac{B_0(B_0+H)^2\mathscr{N}_0(\mathscr{N}_0-1)}{(B_0(\mathscr{N}_0-1)+H\mathscr{N}_0)^2}. \tag{4.6}$$

After the replacement of B^* given by (4.4) and P^* displayed in (4.6), we recover the expressions for V^* and Z^* in terms of $\mathscr{N}_0$ as follows:

$$V^* = \frac{\phi(1-\pi)rH}{(\mu+\alpha)K}\frac{B_0^2(B_0+H)(\mathscr{N}_0-1)}{(B_0(\mathscr{N}_0-1)+H\mathscr{N}_0)^2} \tag{4.7}$$

and

$$Z^* = \frac{\pi(\mu+\alpha)+\phi(1-\pi)rH}{(\mu+\gamma)(\mu+\alpha)K}\frac{B_0^2(B_0+H)(\mathscr{N}_0-1)}{(B_0(\mathscr{N}_0-1)+H\mathscr{N}_0)^2} \tag{4.8}$$

Hence the existence of a unique EPE for the model (2.4), whenever $\mathscr{N}_0 > 1$. The following result gives the existence of equilibria and examines the local stability of the EFE and the PFE.

PROPOSITION 4.1 The following statements hold true:
i) The EFE E_0 is always unstable.
ii) The PFE E_1 of the system (2.4) is LAS whenever $\mathscr{N}_0 < 1$, and the stable manifold of the PFE is $W_s(E_1) = \{(B,V,P) \in \Omega,\ B = B_0\}$.
iii) The PFE is unstable whenever $\mathscr{N}_0 > 1$, and there exists a unique EPE E^* of the system (2.4).

Proof : The Jacobian matrix at E_0 is

$$J(E_0) = \begin{pmatrix} \frac{r}{K}B_0 & 0 & 0 \\ 0 & -(\mu+\alpha) & 0 \\ 0 & \theta\alpha & -\delta \end{pmatrix}.$$

Clearly, rB_0/K is a positive eigenvalue of $J(E_0)$, thus E_0 is unconditionally unstable.
The Jacobian matrix at the PFE E_1 is

$$J(E_1) = \begin{pmatrix} -\frac{r}{K}B_0 & 0 & -f(B_0) \\ 0 & -(\mu+\alpha) & \phi(1-\pi)f(B_0) \\ 0 & \theta\alpha & \theta\pi f(B_0)-\delta \end{pmatrix}.$$

It is clear that $-rB_0/K$ is an eigenvalue of $J(E_1)$, the local stability of PFE is completely determined by the determinant and the trace of the following (2×2)-matrix.

$$J_0 = \begin{pmatrix} -(\mu+\alpha) & \phi(1-\pi)f(B_0) \\ \theta\alpha & \theta\pi f(B_0)-\delta \end{pmatrix}.$$

Straightforward computations show that the determinant and the trace of J_0 are respectively:

$$\det(J_0) = \delta(\mu+\alpha)(1-\mathscr{N}_0), \quad \mathrm{tr}(J_0) = -(\mu+\alpha)-\delta\,(1-\mathscr{N}_{0V})\,. \tag{4.9}$$

If $\mathscr{N}_0 < 1$, then $\det J_0 > 0$ and $\mathscr{N}_{0V} < 1$, which implies that $\mathrm{tr}(J_0) < 0$. Thus the LAS of the PFE. It is not difficult to see that the stable manifold of E_1 is $W_s(E_1)$ defined above. On the other hand, if $\mathscr{N}_0 > 1$, then $\det(J_0) < 0$, and the EFE is unstable. □

We now focus on the global stability of the PFE E_1. To this end, we set:

$$n(B) = B\left\{r - \mu - \frac{rB}{K}\right\} = \frac{r}{K}B(B_0 - B) \quad \text{and} \quad f(B) = \frac{\beta B}{B+H}. \tag{4.10}$$

PROPOSITION 4.2 The PFE is GAS in $\Omega \setminus \{E_0\}$ whenever $\mathscr{N}_0 < 1$.

Proof : We consider the following Lyapunov function

$$L_0(B,V,P) = \left(\frac{(1-\pi)\phi\theta\alpha}{\delta(\mu+\alpha)} + \frac{\theta\pi}{\delta}\right)\int_{B_0}^{B}\frac{f(x)-f(B_0)}{f(x)}dx + \frac{\theta\alpha}{\delta(\mu+\alpha)}V + \frac{1}{\delta}P. \tag{4.11}$$

We now compute the derivative of L along the solution of (2.4). One has

$$\frac{dL_0}{dt} = \left(\frac{(1-\pi)\phi\theta\alpha}{\delta(\mu+\alpha)} + \frac{\theta\pi}{\delta}\right)\left(1 - \frac{f(B_0)}{f(B)}\right)\dot{B} + \frac{\theta\alpha}{\delta(\mu+\alpha)}\dot{V} + \frac{1}{\delta}\dot{P}.$$

Using the expressions of derivatives in (2.4) yields

$$\begin{aligned}
\frac{dL_0}{dt} &= \left(\frac{(1-\pi)\phi\theta\alpha}{\delta(\mu+\alpha)} + \frac{\theta\pi}{\delta}\right)\left(\frac{f(B)-f(B_0)}{f(B)}\right)(n(B) - f(B)P) \\
&+ \frac{\theta\alpha}{\delta(\mu+\alpha)}((1-\pi)\phi f(B)P - (\mu+\alpha)V) + \frac{1}{\delta}(\theta\pi f(B)P + \theta\alpha V - \delta P) \qquad (4.12)\\
&= \left(\frac{(1-\pi)\phi\theta\alpha}{\delta(\mu+\alpha)} + \frac{\theta\pi}{\delta}\right)\left(\frac{f(B)-f(B_0)}{f(B)}\right)n(B) + \left(\frac{(1-\pi)\phi\theta\alpha}{\delta(\mu+\alpha)} + \frac{\theta\pi}{\delta}\right)f(B_0)P - P \\
&= \left(\frac{(1-\pi)\phi\theta\alpha}{\delta(\mu+\alpha)} + \frac{\theta\pi}{\delta}\right)\left(\frac{f(B)-f(B_0)}{f(B)}\right)n(B) + \left(\frac{(1-\pi)\phi\theta\alpha f(B_0)}{\delta(\mu+\alpha)} + \frac{\theta\pi f(B_0)}{\delta} - 1\right)P \\
&= \frac{r}{K}\left(\frac{(1-\pi)\phi\theta\alpha}{\delta(\mu+\alpha)} + \frac{\theta\pi}{\delta}\right)\left(\frac{f(B)-f(B_0)}{f(B)}\right)B(B_0 - B) + P(\mathscr{N}_0 - 1).
\end{aligned}$$

Since f is increasing, $\mathscr{N}_0 < 1$ and $(B,V,P) \in \Omega \setminus \{E_0\}$, we have $dL_0/dt \leqslant 0$. Moreover, the set in $\Omega \setminus \{E_0\}$ such that $dL_0/dt \leqslant 0 = 0$ is $\mathscr{E} = \{(B,V,P) \in \Omega \setminus \{E_0\}; B = B_0,\ P = 0\}$. Replacing P by zero in the second equation of (2.4) leads to $\lim_{t\to+\infty} V(t) = 0$. Thus, largest invariant set contained in $\mathscr{E}$ is the singleton PFE, and the application of LaSalle's Invariant Principle (see LaSalle J. P. (1976)), proves that the PFE is GAS in $\Omega \setminus \{E_0\}$. □

4.2 *Increasing the value of the basic offspring number purifies the environment*

We use the expressions obtained in (4.4), (4.6) and (4.2) to investigate on the behavior of the EPE versus the basic offspring number. First, note that whenever $\mathscr{N}_0 > 1$, the denominators of B^*, V^* and P^* cannot vanish. Recall from (4.4) that

$$B^*(\mathscr{N}_0) = \frac{HB_0}{B_0(\mathscr{N}_0 - 1) + H\mathscr{N}_0},$$

so that $B^*(1) = B_0$, $\lim_{\mathscr{N}_0\to\infty} B^*(\mathscr{N}_0) = 0$, and $\dfrac{\partial B^*}{\partial \mathscr{N}_0} = -\dfrac{HB_0(B_0+H)}{((B_0+H)\mathscr{N}_0 - B_0)^2}$. Thus, B^* is decreasing for $\mathscr{N}_0 > 1$, and tends to zero whenever $\mathscr{N}_0$ tends to $+\infty$.

Similarly, from (4.7), we have

$$V^*(\mathscr{N}_0) = \frac{\phi(1-\pi)rH}{(\mu+\alpha)K}\frac{B_0^2(B_0+H)(\mathscr{N}_0-1)}{(B_0(\mathscr{N}_0-1)+H\mathscr{N}_0)^2},$$

$V^*(1)=0$, and $\lim_{\mathscr{N}_0\to\infty} V^*(\mathscr{N}_0)=0$, and $\dfrac{\partial V^*}{\partial \mathscr{N}_0} = \dfrac{\phi(1-\pi)rHB_0^2(B_0+H)}{(\mu+\alpha)K}\dfrac{[-(B_0+H)\mathscr{N}_0+B_0+2H]}{(B_0(\mathscr{N}_0-1)+H\mathscr{N}_0)^3}$.
Hence, V^* assumes the maximum value at

$$\mathscr{N}_0^m = 1+\frac{H}{B_0+H},$$

giving by

$$V^*_{max} = \frac{\phi(1-\pi)rHB_0^2(B_0+H)}{4H(\mu+\alpha)K}.$$

Precisely, V^* is increasing on $1 \leqslant \mathscr{N}_0 < \mathscr{N}_0^m$, and decreasing whenever $\mathscr{N}_0 > \mathscr{N}_0^m$ and tends to zero. Remember that from (4.6), one has

$$P^*(\mathscr{N}_0) = \frac{rH}{\beta K}\frac{B_0(B_0+H)^2\mathscr{N}_0(\mathscr{N}_0-1)}{(B_0(\mathscr{N}_0-1)+H\mathscr{N}_0)^2}.$$

$P^*(1)=0$, $\lim_{\mathscr{N}_0\to\infty} P^*(\mathscr{N}_0) = \dfrac{rHB_0}{\beta K}$, and $\dfrac{\partial P^*}{\partial \mathscr{N}_0} = \dfrac{rB_0(B_0+H)^2}{\beta KH}\dfrac{1}{(B_0(\mathscr{N}_0-1)+H\mathscr{N}_0)^2}$.
Consequently, P^* is an increasing but saturated function which assumes a maximum value

$$P^*_{max} = \frac{rHB_0}{\beta K} = \frac{(r-\mu)H}{\beta}.$$

On the other hand, thanks to (4.8),

$$Z^*(\mathscr{N}_0) = \frac{\pi(\mu+\alpha)+\phi(1-\pi)rH}{(\mu+\gamma)(\mu+\alpha)K}\frac{B_0^2(B_0+H)(\mathscr{N}_0-1)}{(B_0(\mathscr{N}_0-1)+H\mathscr{N}_0)^2},$$

so that, $Z^*(1)=0$, and $\lim_{\mathscr{N}_0\to\infty} Z^*(\mathscr{N}_0)=0$, and
$\dfrac{\partial V^*}{\partial \mathscr{N}_0} = \dfrac{\pi(\mu+\alpha)+\phi(1-\pi)rHB_0^2(B_0+H)}{(\mu+\alpha)K}\dfrac{[-(B_0+H)\mathscr{N}_0+B_0+2H]}{(B_0(\mathscr{N}_0-1)+H\mathscr{N}_0)^3}$.
Thus, Z^*, has a maximum value at $\mathscr{N}_0^m$, giving by

$$Z^*_{max} = \frac{(\pi(\mu+\alpha)+\phi(1-\pi))\,rHB_0^2(B_0+H)}{4H(\mu+\alpha)K}.$$

Thus, Z^* is increasing on $1 \leqslant \mathscr{N}_0 < \mathscr{N}_0^m$, and decreasing whenever $\mathscr{N}_0 > \mathscr{N}_0^m$, and finally vanishes when $\mathscr{N}_0 \to +\infty$. From these investigations which are illustrated by Figure 5, one can derive the following remark.

REMARK 4.1 The threshold value $\mathscr{N}_0^m$ is the minimum value of the basic offspring number $\mathscr{N}_0$ required to ensure exponential decrease of the all bacterial populations to zero, thus purifying the environment by keeping alive only the population of phages. Fortunately $\mathscr{N}_0^m$ is small enough ($1 < \mathscr{N}_0^m < 2$), so that, not too much effort is needed to achieve this value in order to purify the environmental reservoir of bacteria.

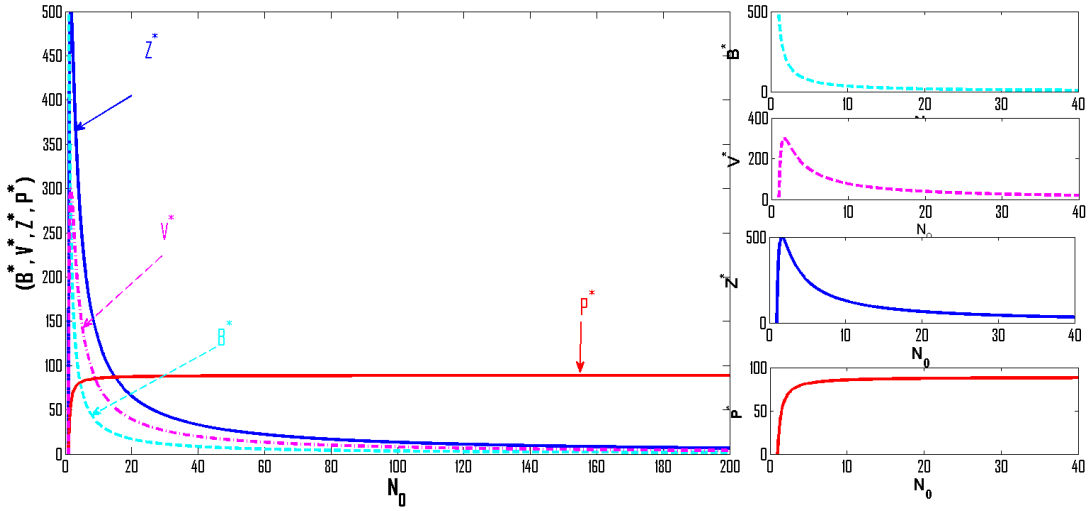

FIG. 5. Graphs of B^*, V^*, Z^* and P^* versus $\mathcal{N}_0$: On the left panel, one can observe that the bacteria subpopulations B^*, V^*, Z^* go extinct, while the population of phages sustains for large value of the basic offspring number $\mathcal{N}_0$. On the right panel, we zoom the figure in the left panel so that one can numerically see that the populations of V^* and Z^* assume their maximum values at the same threshold value $\mathcal{N}_0^m$.

The following theorem specifies the type of the PFE based on the values or ranges of the basic offspring number $\mathcal{N}_0$.

THEOREM 4.1 For the system (2.4), the PFE is
i) an attracting node if $\mathcal{N}_0 < 1$,
ii) a hyperbolic saddle if $\mathcal{N}_0 > 1$,
iii) a saddle-node if $\mathcal{N}_0 = 1$.

Proof : The characteristic polynomial of the Jacobian matrix at the PFE denoted by $J(E_1)$ has the form

$$P(\lambda) = \left(\lambda + \frac{r}{K}B_0\right)\left(\lambda^2 - tr(J_0)\lambda + \det(J_0)\right) \tag{4.13}$$

where $\mathrm{tr}(J_0)$ and $\det(J_0)$ are given in Eq. (4.9).

i) For $\mathcal{N}_0 < 1$, $\det(J_0) > 0$ and using the Descartes's rule sign, the roots of (4.13) are reals and negative. Thus the PFE in an attracting node.

ii) For $\mathcal{N}_0 > 1$, $\det(J_0) < 0$, and there exists three real eigenvalues with at least one positive. Thus the PFE is hyperbolic saddle.

iii) For $\mathcal{N}_0 = 1$, the eigenvalues of the Jacobian matrix of (2.4) at PFE are $-rK/B_0$, $\mathrm{tr}(J_0)$ and 0. Recalling that $\mathrm{tr}(J_0) = -(\mu+\alpha) - \delta(1-\mathcal{N}_{0_V}) < 0$, then, PFE is a non-hyperbolic critical point with two negative eigenvalue and one simple zero eigenvalue. Thus, the center manifold theory approximation applies in order to determine its stability.

Let's adopt the change of variables $U = B - B_0$, $V = V$, $W = P$ and set $X = (U, V, W)^T$ such that the

system (2.4) has the form

$$\frac{dX}{dt} = AX + F(U,V,W), \tag{4.14}$$

where,

$$A = \begin{pmatrix} -rB_0/K & 0 & -f(B_0) \\ 0 & -(\mu+\alpha) & \phi(1-\pi)f(B_0) \\ 0 & \theta\alpha & \theta\pi f(B_0) - \delta \end{pmatrix}$$

and

$$F(U,V,W) = \begin{pmatrix} -rU^2/K - \dfrac{\beta HU}{(U+B_0+H)(B_0+H)}W \\ \phi(1-\pi)\dfrac{\beta HU}{(U+B_0+H)(B_0+H)}W \\ \theta\pi\dfrac{\beta HU}{(U+B_0+H)(B_0+H)}W \end{pmatrix}.$$

Using Taylor expansion around $(0,0,0)$, we obtain F as follows

$$F(U,V,W) = \begin{pmatrix} -rU^2/K - \dfrac{\beta H}{(B_0+H)}UW + O(U^2) \\ \phi(1-\pi)\dfrac{\beta H}{(B_0+H)}UW + O(U^2) \\ \theta\pi\dfrac{\beta H}{(B_0+H)}UW + O(U^2) \end{pmatrix}.$$

In order to diagonalize the linear part of the system (4.14), we set

$$\eta = \frac{\beta B_0 K}{rB_0(B_0+H) - K(\alpha+\mu+\delta)(B_0+H) + K\theta\pi\beta B_0},$$

and consider the matrix P of the eigenvectors of $J(E_1)$ given by

$$P = \begin{pmatrix} 1 & \eta & \dfrac{\beta K}{r(B_0+H)} \\ 0 & -\dfrac{(\mu+\alpha)}{\theta\alpha} & \dfrac{\phi(1-\pi)f(B_0)}{\alpha+\mu} \\ 0 & 1 & 1 \end{pmatrix}.$$

Then,

$$P^{-1}AP = \mathscr{B} = \operatorname{diag}\left(-rB_0/K, -(\mu+\alpha) - \delta\left(1-\mathscr{N}_{0_V}\right), 0\right).$$

Using the transformation $Y = PX$, where $Y = (B,V,P)^T$ we have

$$\frac{dY}{dt} = \mathscr{B}Y + P^{-1}FPY$$

and the system (4.14) takes the form

$$\begin{cases} \dfrac{dB}{dt} = -rB_0B/K + O(|\,B,V,P\,|^2), \\ \dfrac{dV}{dt} = -\left(\mu+\alpha+\delta\left(1-\mathscr{N}_{0_V}\right)\right)V + O(|\,B,V,P\,|^2), \\ \dfrac{dP}{dt} = 0 + g_3(B,V,P), \end{cases} \tag{4.15}$$

where,

$$\begin{aligned} g_3(B,V,P) &= \frac{K\beta^2(\mu+\alpha)\left(\theta\alpha(1-\pi)\phi+\theta\pi(\mu+\alpha)\right)}{r(B_0+H)\left(\theta\alpha(1-\pi)\beta B_0+(\alpha+\mu)^2(B_0+H)\right)} \\ &+ \left(B+\frac{\beta B_0}{\frac{r}{K}B_0(B_0+H)-((\alpha+\mu)+\delta(1-\mathscr{N}_{0V}))}V+\beta\frac{K}{r(B_0+H)}P\right)(V+P). \end{aligned}$$

Then the application of the center manifold theory yields the following system

$$\begin{cases} \dfrac{dB}{dt} = -rB_0B/K + O(|\,B,V,P\,|^2), \\ \dfrac{dV}{dt} = -\left(\mu+\alpha+\delta\left(1-\mathscr{N}_{0_V}\right)\right)V + O(|\,B,V,P\,|^2), \\ \dfrac{dP}{dt} = \nu P^2 + O(P^3), \end{cases} \tag{4.16}$$

where,

$$\nu = \frac{K\beta^2(\mu+\alpha)\left(\theta\alpha(1-\pi)\phi+\theta\pi(\mu+\alpha)\right)}{r(B_0+H)\left(\theta\alpha(1-\pi)\beta B_0+(\alpha+\mu)^2(B_0+H)\right)}.$$

Since $\nu > 0$, the PFE is a saddle node. □

The global stability result established in Theorem 4.2 is illustrated numerically by Figure 6, where the trajectories of the model (2.4) are plotted for different initial conditions and $\mathscr{N}_0 = 0.409$. We observe that susceptible bacteria population persists, while lysogen bacteria and free phage populations vanish.

REMARK 4.2 The instability of the EFE $E_0 = (0,0,0)$ predicts that the phages and bacteria cannot simultaneously face extinction, and justify the fact that phages feed on bacteria only and do not consume other resources. Thus in the absence of bacteria, phages are condemned to elimination.

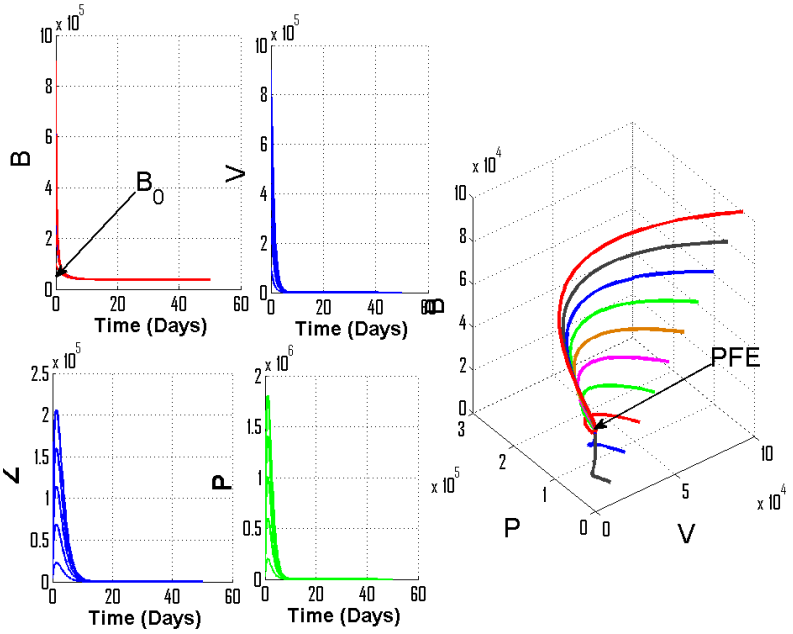

FIG. 6. Global asymptotic stability of PFE E_1 whenever $\mathcal{N}_0 = 0,409$.

4.3 *Existence of Hopf Bifurcation around the EPE*

Our purpose here is to determine the conditions under which model (2.4) undergoes a Hopf bifurcation and illustrate it numerically. The Jacobian matrix of (2.4) evaluated at E^* is

$$J(E^*) = \begin{pmatrix} r-\mu-2rB^*/K-\dfrac{\beta P^* H}{(B^*+H)^2} & 0 & -\dfrac{\beta B^*}{B^*+H} \\ \dfrac{\phi(1-\pi)\beta P^* H}{(B^*+H)^2} & -(\mu+\alpha) & \phi(1-\pi)\dfrac{\beta B^*}{B^*+H} \\ \dfrac{\theta\pi\beta P^* H}{(B^*+H)^2} & \theta\alpha & \theta\pi\dfrac{\beta B^*}{B^*+H}-\delta \end{pmatrix}.$$

Knowing that at the EPE point E^*, one has

$$\frac{\theta\pi\beta B^*}{B^*+H}-\delta = -\frac{\theta\alpha(1-\pi)\phi\beta B^*}{(\mu+\alpha)(B^*+H)},\ P^* = \frac{r}{\beta K}(B_0-B^*)(B^*+H),\ r-\mu-2rB^*/K = r(B_0-2B^*)/K,$$

$J(E^*)$ becomes,

$$J(E^*) = \begin{pmatrix} r(B_0-2B^*)/K - \dfrac{r}{K}\dfrac{(B_0-B^*)H}{(B^*+H)} & 0 & -\dfrac{\beta B^*}{B^*+H} \\ \phi(1-\pi)\dfrac{r}{K}\dfrac{(B_0-B^*)H}{(B^*+H)} & -(\mu+\alpha) & \phi(1-\pi)\dfrac{\beta B^*}{B^*+H} \\ \theta\pi\dfrac{r}{K}\dfrac{(B_0-B^*)H}{(B^*+H)} & \theta\alpha & -\dfrac{\theta\alpha(1-\pi)\phi\beta B^*}{(\mu+\alpha)(B^*+H)} \end{pmatrix}.$$

The characteristic polynomial of $J(E^*)$ is

$$P(\lambda) = \lambda^3 + a_2(B^*)\lambda^2 + a_1(B^*)\lambda + a_0(B^*), \tag{4.17}$$

where,

$$\begin{aligned} a_2(B^*) &= -\frac{r}{K}(B_0-2B^*) + \frac{\theta\alpha(1-\pi)\phi\beta B^*}{(\mu+\alpha)(B^*+H)} + \frac{r}{K}\frac{(B_0-B^*)H}{(B^*+H)} + (\mu+\alpha), \\ a_1(B^*) &= \frac{r}{K}(B_0-2B^*)\left(\frac{\theta\alpha\phi(1-\pi)\beta B^*}{(\mu+\alpha)(B^*+H)} + (\mu+\alpha)\right) + (\mu+\alpha+\delta)\frac{rH}{K}\frac{(B_0-B^*)}{(B^*+H)}, \\ a_0(B^*) &= \frac{rH\delta(\mu+\alpha)}{K(B^*+H)}(B_0-B^*). \end{aligned} \tag{4.18}$$

It follows from the Routh-Hurwitz criteria (see Birkhoff G. & Rota G.C. (1989)) that E^* is LAS if and only if $a_2(B^*) > 0$, $a_0(B^*) > 0$ and,

$$Q(B^*) = a_1(B^*)a_2(B^*) - a_0(B^*) > 0. \tag{4.19}$$

Plugging (4.18) into (4.19) yields

$$\begin{aligned} Q(B^*) &= -\frac{r}{K}(B_0-2B^*)\left\{1 + (1+\mu+\alpha)\frac{\theta\alpha(1-\pi)\phi\beta B^*}{(\mu+\alpha)(B^*+H)} + (\mu+\alpha)(1+\mu+\alpha)\right\} \\ &+ \frac{\theta\alpha\phi(1-\pi)\beta B^*}{(\mu+\alpha)(B^*+H)} + \frac{rH(B_0-B^*)}{K(B^*+H)}\left(1 + (\mu+\alpha+\delta) + (\mu+\alpha)^2\right). \end{aligned} \tag{4.20}$$

After direct but simple computations, (4.18) becomes,

$$\begin{aligned} a_2(B^*) &= \frac{2r(\mu+\alpha)B^{*2} + \left[rH(\mu+\alpha)(\mathscr{N}_0-1) + \theta\alpha(1-\pi)\phi\beta + (\mu+\alpha)^2K\right]B^* + (\mu+\alpha)^2KH}{K(\mu+\alpha)(B^*+H)}, \\ a_1(B^*) &= \frac{r}{K}(B_0-2B^*)\left(\frac{\theta\alpha\phi(1-\pi)\beta B^*}{(\mu+\alpha)(B^*+H)} + (\mu+\alpha)\right) + (\mu+\alpha+\delta)\frac{rH}{K}\frac{(B_0-B^*)}{(B^*+H)}, \\ a_0(B^*) &= \frac{rH\delta(\mu+\alpha)}{K(B^*+H)}\frac{B_0(B_0+H)(\mathscr{N}_0-1)}{(B_0(\mathscr{N}_0-1)+H\mathscr{N}_0)}, \end{aligned} \tag{4.21}$$

and

$$Q(B^*) = \frac{B^*\left(\tau_3 B^{*3} + \tau_2 B^{*2} + \tau_1 B^* + \tau_0\right)}{K^2(\mu+\alpha)^2(B^*+H)^2}, \tag{4.22}$$

where,

$$\begin{aligned}
&\tau_3 = 4r^2(\mu+\alpha)\left(\theta\alpha(1-\pi)\phi\beta+(\mu+\alpha)^2\right) > 0,\\
&\tau_2 = 2\delta(\mu+\alpha)r^2H\left(\theta\alpha(1-\pi)\phi\beta+(\mu+\alpha)^2\right) - 2r\left[\theta\alpha(1-\pi)\phi\beta+(\mu+\alpha)^2\right]\tau_0,\\
&\tau_1 = 2r^2(\mu+\alpha)^2\delta HB_0 + 2K(\mu+\alpha)^2rH\left[\theta\alpha(1-\pi)\phi\beta+(\mu+\alpha)^2\right]\\
&+\left[r(\mu+\alpha)H + K\theta\alpha(1-\pi)\phi\beta - r(\mu+\alpha)B_0\right]\\
&\times\left[r(\mu+\alpha)^2H - \theta\alpha(1-\pi)\phi\beta B_0 - r(\mu+\alpha)^2B_0 - (\mu+\alpha)H\right],\\
&\tau_0 = -K(\mu+\alpha)^2H\left[rH(\mu+\alpha)^2 + r\theta\alpha(1-\pi)\phi\beta B_0 + r(\mu+\alpha)^2B_0\right] + \delta(\mu+\alpha)^2r^2HB_0^2(1-\mathscr{N}_0).
\end{aligned} \tag{4.23}$$

From (4.21), $a_2(B^*) > 0$, and $a_0(B^*) > 0$. The number and the signs of the roots of $Q(B^*)$ depend on the number and the signs of the following polynomial

$$q(B^*) = \tau_3 {B^*}^3 + \tau_2 {B^*}^2 + \tau_1 B^* + \tau_0. \tag{4.24}$$

We use the Descartes's rule of signs to investigate the number of positive roots of Eq. (4.24). We note from Eq.(4.20) that $Q(B^*) > 0$ for all $B^* \geqslant B_0/2$, possible roots B_c^* of $q(B^*)$ lie on the interval $(0, B_0/2)$. From Eq. (4.24) and the fact that $\mathscr{N}_0 > 1$ we conclude that $q(0) = \tau_0 < 0$. Using Eq. (4.20), one has $Q(B_0/2) > 0$, the intermediate value theorem guarantees the existence of at least one root of $q(B^*)$ in $(0, B_0/2)$. Moreover, $\tau_3 > 0$ and $\tau_0 < 0$ imply that $\tau_2 \geqslant 0$. Thus, regardless the sign of τ_1, Descartes's rule of signs guarantees the existence of at most one positive root of $q(B^*)$. Hence the existence of a unique root B_c^* of Eq. (4.24).

Moreover, note that from Eq. (4.4), one has

$$\mathscr{N}_0 = \frac{B_0(B^*+H)}{B^*(B_0+H)}, \tag{4.25}$$

so that

$$B^* = \frac{HB_0}{B_0(\mathscr{N}_0-1)+H\mathscr{N}_0} = B_c^* \Longleftrightarrow \mathscr{N}_0 = \mathscr{N}_0^c,$$

where,

$$\mathscr{N}_0^c = 1 + \frac{B_0+H}{B_c^*+H}. \tag{4.26}$$

Furthermore,

$$\mathscr{N}_0^c = 1 + \frac{B_0+H}{B_c^*+H} > \frac{B_0+H}{\frac{B_0}{2}+H} = 2 + \frac{B_0}{B_0+2H}.$$

Due to the high degree of the polynomial $q(B^*)$, it is difficult to find the explicit value of $\mathscr{N}_0^c$. Thus, for numerical illustrations, it is impossible to use the value of $\mathscr{N}_0^c$ to test the stability of EPE. Alternatively and equivalently, we will select appropriate parameter sets to obtain numerically the desired signs of $Q(B^*)$.

From the investigations above, it is obvious that $Q(B^*)$ (or equivalently $q(B^*)$) is positive for $\mathscr{N}_0 < \mathscr{N}_0^c$ and negative for $\mathscr{N}_0 > \mathscr{N}_0^c$. Thus, the local stability of the EPE is summarized by the following result:

PROPOSITION 4.3 The EPE E^* is LAS if and only if, $1 < \mathscr{N}_0 < \mathscr{N}_0^c$.

The fact that we have established the LAS (it is even GAS) of PFE for $\mathscr{N}_0 < 1$, its instability for $\mathscr{N}_0 > 1$ and the existence of a positive LAS equilibrium E^* when $\mathscr{N}_0 > 1$, shows that model (2.4) presents a transcritical bifurcation at $\mathscr{N}_0 = 1$ as stated in the following result.

THEOREM 4.2 The model (2.4) exhibits a trans-critical bifurcation at $\mathscr{N}_0 = 1$.

In order to prove the occurrence of Hopf bifurcation. We note that $a_0(B^*)$, $a_2(B^*)$ and $Q(B^*)$ can be expressed as the functions of $\mathscr{N}_0$ which can be chosen as the bifurcation parameter.

THEOREM 4.3 Denote

$$\mathscr{H}_0 = -a_2(\mathscr{N}_0^c)a_1(\mathscr{N}_0^c)a_1'(\mathscr{N}_0^c) - a_2'(\mathscr{N}_0^c)a_1(\mathscr{N}_0^c) + a_0'(\mathscr{N}_0^c). \tag{4.27}$$

Then, the model (2.4) exhibits a Hopf bifurcation at $\mathscr{N}_0 = \mathscr{N}_0^c$ around the EPE if $\mathscr{H}_0 \neq 0$. Moreover, the Hopf bifurcation is supercritical if $\mathscr{H}_0 > 0$ and sub-critical if $\mathscr{H}_0 < 0$.

Proof : We use the method presented in Fahad B., Santanu R. & Ezio V. (2018) to find the analytic conditions for the system (2.4) to undergo a Hopf bifurcation at $\mathscr{N}_0 = \mathscr{N}_0^c$. We set

$$Q(\mathscr{N}_0) = a_1(\mathscr{N}_0)a_2(\mathscr{N}_0) - a_0(\mathscr{N}_0). \tag{4.28}$$

By the condition $Q(\mathscr{N}_0^c) = 0$, the characteristic equation (4.17) $J(E^*)$ of takes the form

$$\left(\lambda^2 + a_1(\mathscr{N}_0^c)\right)\left(\lambda + a_2(\mathscr{N}_0^c)\right) = 0. \tag{4.29}$$

Let ρ_1, ρ_2, and ρ_3, denote the roots of (4.29), such that $\rho_3 = -a_2(\mathscr{N}_0^c) < 0$ and $\rho_1, \rho_2 = \pm i\sqrt{a_1(\mathscr{N}_0^c)}$.

We recall from (4.21) that $a_0(\mathscr{N}_0^c) > 0$, $a_2(\mathscr{N}_0^c) > 0$ and observe that $a_1(\mathscr{N}_0^c) = a_1(B_c^*) > 0$ (because $B_c^* < B_0/2$). Thus, for $\mathscr{N}_0 = \mathscr{N}_0^c$, there are one negative eigenvalue and two purely imaginary eigenvalues of $J(E^*)$.

The general form of ρ_1, ρ_2 in the neighborhood of $\mathscr{N}_0^c$ is $\rho_1 = x + iy$, and $\rho_2 = x - iy$. Based on Chakraborty K., Jana S. & Kar T. K. (2012), we now check the following transversality conditions.

$$\frac{\partial R_e \rho_j(\mathscr{N}_0)}{\partial \mathscr{N}_0} \mid_{\mathscr{N}_0 = \mathscr{N}_0^c} \neq 0 \quad j = 1, 2. \tag{4.30}$$

Substituting $\rho_j = x \pm iy$ into (4.17) and calculating the derivative gives

$$\begin{aligned} L_1(\mathscr{N}_0)\frac{\partial x}{\partial \mathscr{N}_0} - L_2(\mathscr{N}_0)\frac{\partial y}{\partial \mathscr{N}_0} + L_3(\mathscr{N}_0) = 0, \\ L_2(\mathscr{N}_0)\frac{\partial x}{\partial \mathscr{N}_0} + L_1(\mathscr{N}_0)\frac{\partial y}{\partial \mathscr{N}_0} + L_4(\mathscr{N}_0) = 0, \end{aligned} \tag{4.31}$$

where,

$$\begin{aligned} L_1(\mathscr{N}_0) &= 3(x^2 - y^2) + 2a_2(\mathscr{N}_0)x + a_1(\mathscr{N}_0), \\ L_2(\mathscr{N}_0) &= 6xy + 2a_2(\mathscr{N}_0)y, \\ L_3(\mathscr{N}_0) &= \frac{\partial a_2(\mathscr{N}_0)}{\partial \mathscr{N}_0}(x^2 - y^2) + \frac{\partial a_1(\mathscr{N}_0)}{\partial \mathscr{N}_0}x + \frac{\partial a_0(\mathscr{N}_0)}{\partial \mathscr{N}_0} \\ L_4(\mathscr{N}_0) &= 2\frac{\partial a_2(\mathscr{N}_0)}{\partial \mathscr{N}_0}xy + \frac{\partial a_1(\mathscr{N}_0)}{\partial \mathscr{N}_0}y. \end{aligned} \tag{4.32}$$

Straightforward computations solve system (4.31) and yield

$$\begin{aligned}\frac{\partial Re\rho_j(\mathscr{N}_0)}{\partial \mathscr{N}_0}\mid_{\mathscr{N}_0=\mathscr{N}_0^c} &= \frac{\partial x}{\partial \mathscr{N}_0}(\mathscr{N}_0^c)\\ &= -\frac{L_2(\mathscr{N}_0^c)L_4(\mathscr{N}_0^c)+L_1(\mathscr{N}_0^c)L_3(\mathscr{N}_0^c)}{L_1^2(\mathscr{N}_0^c)+L_2^2(\mathscr{N}_0^c)}\\ &= -\frac{a_2(\mathscr{N}_0^c)a_1(\mathscr{N}_0^c)a_1'(\mathscr{N}_0^c)+a_2'(\mathscr{N}_0^c)a_1(\mathscr{N}_0^c)-a_0'(\mathscr{N}_0^c)}{a_1(\mathscr{N}_0^c)+a_2^2(\mathscr{N}_0^c)}\\ &= -\frac{\mathscr{H}_0}{a_1(\mathscr{N}_0^c)+a_2^2(\mathscr{N}_0^c)}. \qquad (4.33)\end{aligned}$$

Since by hypothesis $\mathscr{H}_0 \neq 0$, the transversality conditions (4.30) hold. Hence the existence of Hopf bifurcation. This ends the proof of Theorem 4.3. □

To illustrate the Hopf bifurcation phenomenon in Theorem 4.3 above, we choose two suitable sets of parameter values from Table 1, such that for the first set, $Q(B^*) > 0$ or equivalently $\mathscr{N}_0 < \mathscr{N}_0^c$ (i.e E^* is locally stable) and for the second set, $Q(B^*) < 0$ or equivalently $\mathscr{N}_0 > \mathscr{N}_0^c$ (i.e E^* is unstable and periodic solutions occur, see Figure 8). For the first set, the LAS of E^* is guaranteed and is illustrated in Figure 7.

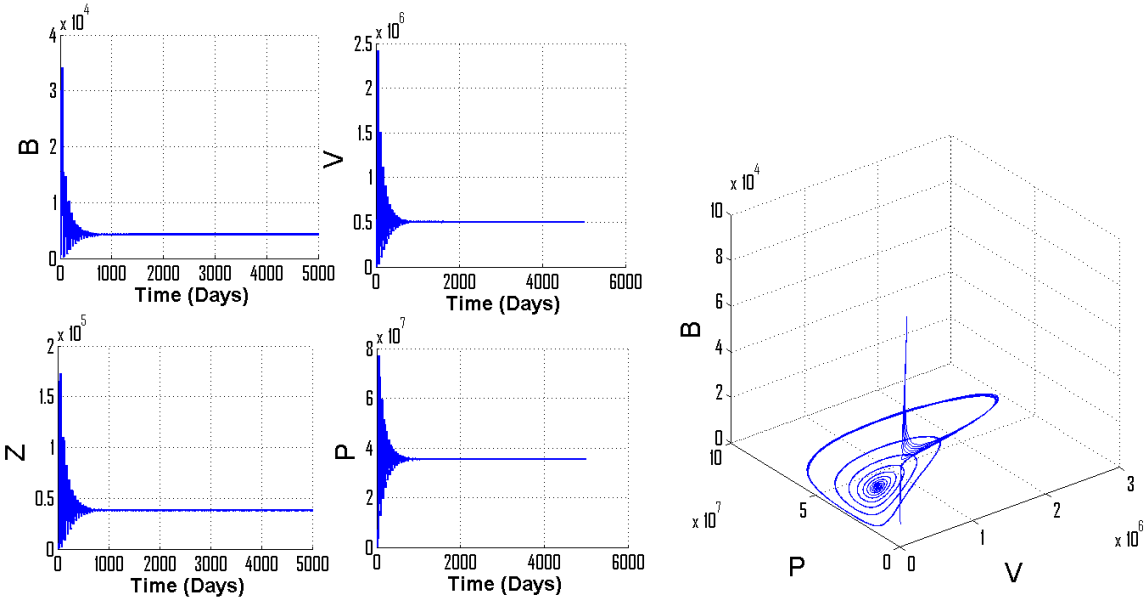

FIG. 7. LAS of the EPE: $\mathscr{N}_0 = \mathbf{1.56}$, $\mathbf{Q(B^*) = 0.17264514 > 0}$. The parameter set is $r = 0.8$, $K = 10^6$, $\mu = 0.5$, $\beta = 0.75$, $H = 10^7$, $\theta = 100$, $\phi = 80$, $\pi = 0.7$, $\alpha = 0.04$ $\gamma = 1$, $\delta = 0.06$, $B_0 = 8.8 \times 10^7$.

For the second set, $Q(B^*) < 0$ such that E^* is unstable and leads to the appearance of periodic oscillations around E^*. From Figure 8, one can easily see that a solution starting in the first orthant approaches

the periodic orbit as time evolves. Actually, Figure 7 and Figure 8 illustrate the Hopf bifurcation at $\mathscr{N}_0 = \mathscr{N}_0^c$, around the EPE.

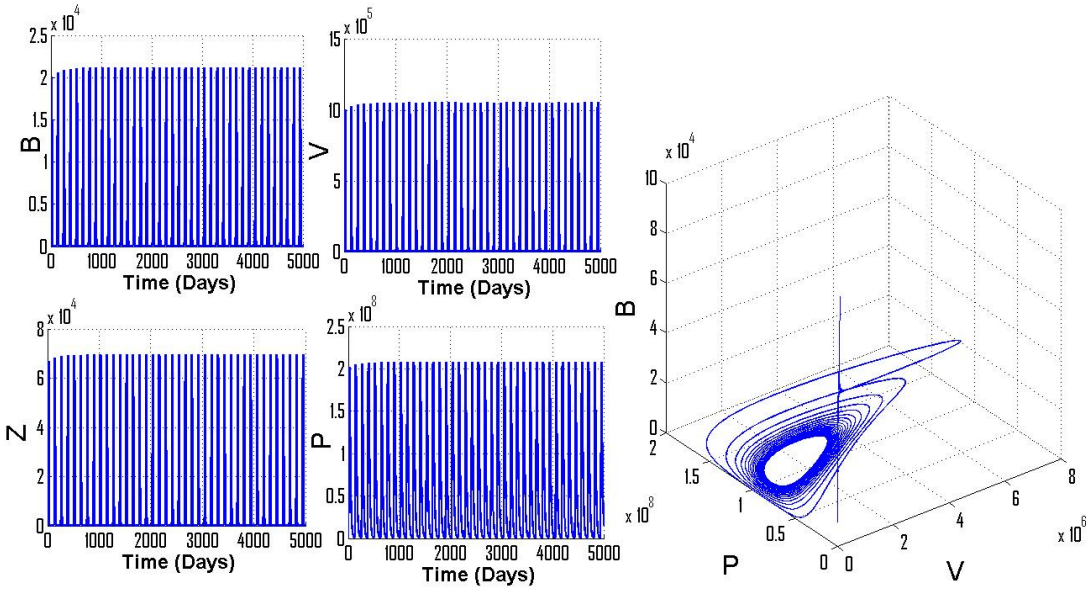

FIG. 8. Periodic solutions for $\mathscr{N}_0 = 4.73$. $\mathbf{Q}(\mathbf{B}^*) = -\mathbf{0.006823032} < \mathbf{0}$. The parameter set is $r = 0.8$, $K = 10^6$, $\mu = 0.15$, $\beta = 0.75$, $H = 10^5$, $\theta = 100$, $\phi = 100$, $\pi = 0.7$, $\gamma = 1$, $\delta = 0.06$. $B_0 = 3.6588 \times 10^7$.

4.4 *Estimation of the basin of attraction of the EPE*

In this paragraph, an estimate of the basin of attraction of the EPE E^* is provided. Note that the existence of stable periodic solutions for model (2.4) precludes the global asymptotic stability of E^* in the entire interior of Ω. We are therefore left with the possibility of finding a subset Ω_{E^*} of Ω containing E^* such that every solution initiated in Ω_{E^*} converges to E^*. Let's denote the stable manifold of E_1 by $W_s(E_1)$, define the quantity

$$B_m = B_0 - B^* = \frac{B_0(B_0+H)(\mathscr{N}_0-1)}{B_0(\mathscr{N}_0-1)+H\mathscr{N}_0} \geqslant 0, \tag{4.34}$$

and the subset

$$\Omega_{E^*} = \left\{ (B,V,P) \in \Omega : B_m \leqslant B(t) \leqslant \frac{\phi r K}{4\mu} \right\} \setminus W_s(E_1).$$

Recall that if one assumes $1 < \mathscr{N}_0 < \mathscr{N}_0^c$, so that $B^* \in \Omega_{E^*}$ is guaranteed, and $Q(B^*) > 0$, then the EPE E^* is LAS. This suggests that the global asymptotic stability can be investigated in Ω_{E^*}. Precisely, we prove in Theorem 4.4 below that Ω_{E^*} is actually contained in the basin of attraction of E^*.

THEOREM 4.4 whenever $1 < \mathscr{N}_0 < \mathscr{N}_0^c$, the EPE E^*, of the system (2.4) is GAS in Ω_{E^*}.

Proof : Note that Ω_{E^*} contains, neither the EFE E_0, nor the PFE E_1. We follow the works in Xiabong T. & Rui X. (2011), Berge T., Lubuma J.M.S., Moremedi G.M., Morris N. & Kondera-Shava

R. (2016), to propose the following Lyapunov function candidate for the EPE.

$$L(B,V,P) = a\int_{B^*}^{B}\frac{f(x)-f(B^*)}{f(B)}dx + b\left(V - V^* - V^*\ln\frac{V}{V^*}\right) + c\left(P - P^* - P^*\ln\frac{P}{P^*}\right), \tag{4.35}$$

where a, b, and c are three positive constants to be determined shortly. We now compute the derivative of L along the solutions of (2.4).

$$\frac{dL}{dt} = a\left(1-\frac{f(B^*)}{f(B)}\right)\frac{dB}{dt} + b\left(1-\frac{V^*}{V}\right)\frac{dV}{dt} + c\left(1-\frac{P^*}{P}\right)\frac{dP}{dt}. \tag{4.36}$$

Substituting the expressions of (2.4) in (4.36) yields

$$\begin{aligned}\frac{dL}{dt} &= a\left(1-\frac{f(B^*)}{f(B)}\right)(n(B)-f(B)P) + b\left(1-\frac{V^*}{V}\right)((1-\pi)\phi f(B)P-(\mu+\alpha)V)\\ &+ c\left(1-\frac{P^*}{P}\right)(\theta\pi f(B)P+\theta\alpha V-\delta P).\end{aligned}$$

Straightforward calculations give

$$\begin{aligned}\frac{dL}{dt} &= a\left(1-\frac{f(B^*)}{f(B)}\right)(n(B)-n(B^*)-f(B)P+f(B^*)P^*)\\ &+ b\left(1-\frac{V^*}{V}\right)\left((1-\pi)\phi f(B)P-(1-\pi)\phi f(B^*)P^*\frac{V}{V^*}\right)\\ &+ c\left(1-\frac{P^*}{P}\right)\left(\theta\pi f(B)P+\theta\alpha V-\theta\pi f(B^*)P-\theta\alpha V^*\frac{P}{P^*}\right).\end{aligned}$$

Further expansions yield,

$$\begin{aligned}\frac{dL}{dt} &= a\left(\frac{f(B)-f(B^*)}{f(B)}\right)(n(B)-n(B^*)) - af(B)P + af(B^*)P + af(B^*)P^* - a\frac{f(B^*)^2}{f(B)}P^*\\ &+ b(1-\pi)\phi f(B)P - b(1-\pi)\phi f(B^*)P^*\frac{V}{V^*} - b(1-\pi)\phi f(B)P\frac{V}{V^*} + b(1-\pi)\phi f(B^*)P^*\\ &+ c\theta\pi f(B)P + c\theta\alpha V - c\theta\pi f(B^*)P - c\theta\alpha V^*\frac{P}{P^*}P - c\theta\pi f(B)P^* - c\theta\alpha\frac{P^*}{P}V\\ &+ c\theta\pi f(B^*)P^* + c\theta\alpha V^*.\end{aligned}$$

After grouping the terms of the above expression, we have,

$$\begin{aligned}\frac{dL}{dt} &= a\left(\frac{f(B)-f(B^*)}{f(B)}\right)(n(B)-n(B^*)) + f(B)P(-a+b(1-\pi)\phi)) + f(B^*)P^*(a+b(1-\pi)\phi)\\ &- a\frac{f(B^*)^2}{f(B)}P^* + \left[-b(1-\pi)\phi f(B^*)\frac{P^*}{V^*} + c\theta\alpha\right]V + \left[af(B^*) - c\theta\alpha\frac{V^*}{P^*} - c\theta\pi f(B^*)\right]P\\ &- c\theta\pi f(B)P^* - c\theta\alpha\frac{P^*}{P}V + c\theta\pi f(B^*)P^* + c\theta\alpha V - b(1-\pi)\phi f(B)P\frac{V}{V^*}.\end{aligned}$$

Now, choose a, b, and c such that the expressions in the brackets vanish, that is

$$\begin{aligned}&af(B^*) - c\theta\alpha\frac{V^*}{P^*} - c\theta\pi f(B^*) = 0,\\ &-b(1-\pi)\phi f(B^*)\frac{P^*}{V^*} + c\theta\alpha = 0.\end{aligned} \tag{4.37}$$

Fix $c>0$ and pose

$$a=\left(\frac{\theta\alpha V^*}{f(B^*)P^*}+\theta\pi\right)c,\ b=\frac{\theta\alpha V^*}{(1-\pi)\phi f(B^*)P^*}c.$$

Then, the derivative of L along the trajectories of (2.4) becomes,

$$\begin{aligned}\frac{dL}{dt} &= c\left(\frac{\theta\alpha V^*}{f(B^*)P^*}+\theta\pi\right)\left(\frac{f(B)-f(B^*)}{f(B)}\right)(n(B)-n(B^*))-c\theta\alpha V^*\frac{f(B^*)}{f(B)}\\ &+ f(B^*)P^*\left(\frac{\theta\alpha V^*}{f(B^*)P^*}c+\theta\pi c+\frac{\theta\alpha V^*}{f(B^*)P^*}c\right)-c\theta\pi f(B^*)P^*\frac{f(B^*)}{f(B)}-c\theta\pi f(B)P^*\\ &- c\theta\alpha V\frac{P^*}{P}-c\theta\alpha V^*\frac{f(B)PV^*}{f(B^*)P^*V}+c\theta\pi f(B^*)P^*+c\theta\alpha V^*\\ &= c\left(\frac{\theta\alpha V^*}{f(B^*)P^*}+\theta\pi\right)\left(\frac{f(B)-f(B^*)}{f(B)}\right)(n(B)-n(B^*))+3c\theta\alpha V^*+2c\theta\pi f(B^*)P^*\\ &- c\theta\alpha V^*\frac{f(B^*)}{f(B)}-c\theta\pi f(B^*)P^*\frac{f(B^*)}{f(B)}-c\theta\pi f(B)P^*-c\theta\alpha V\frac{P^*}{P}-c\theta\alpha V^*\frac{f(B)PV^*}{f(B^*)P^*V}.\end{aligned}$$

Further rearrangements lead us to

$$\begin{aligned}\frac{dL}{dt} &= c\left(\frac{\theta\alpha V^*}{f(B^*)P^*}+\theta\pi\right)\left(\frac{f(B)-f(B^*)}{f(B)}\right)(n(B)-n(B^*))+c\theta\pi f(B^*)P^*\left(2-\frac{f(B^*)}{f(B)}-\frac{f(B)}{f(B^*)}\right)\\ &+ c\theta\alpha V^*\left(3-\frac{f(B^*)}{f(B)}-\frac{f(B)PV^*}{f(B^*)P^*V}-\frac{VP^*}{V^*P}\right)\\ &= c\left(\frac{\theta\alpha V^*}{f(B^*)P^*}+\theta\pi\right)\frac{\beta(B-B^*)^2}{(B+H)(B^*+H)}\left(r-\mu-\frac{r}{K}(B+B^*)\right)\\ &+ c\theta\alpha V^*\left(3-\frac{f(B^*)}{f(B)}-\frac{f(B)PV^*}{f(B^*)P^*V}-\frac{VP^*}{V^*P}\right)+c\theta\pi f(B^*)P^*\left(2-\frac{f(B^*)}{f(B)}-\frac{f(B)}{f(B^*)}\right).\end{aligned}$$

The gathering of some suitably selected terms yields

$$\begin{aligned}\frac{dL}{dt} &= -c\frac{r}{K}\left(\frac{\theta\alpha V^*}{f(B^*)P^*}+\theta\pi\right)\frac{\beta(B-B^*)^2}{(B+H)(B^*+H)}(B-(B_0-B^*))\\ &+ c\theta\alpha V^*\left(3-\frac{f(B^*)}{f(B)}-\frac{f(B)PV^*}{f(B^*)P^*V}-\frac{VP^*}{V^*P}\right)+c\theta\pi f(B^*)P^*\left(2-\frac{f(B^*)}{f(B)}-\frac{f(B)}{f(B^*)}\right)\\ &= -c\frac{r}{K}\left(\frac{\theta\alpha V^*}{f(B^*)P^*}+\theta\pi\right)\frac{\beta(B-B^*)^2}{(B+H)(B^*+H)}(B-B_m)\\ &+ c\theta\alpha V^*\left(3-\frac{f(B^*)}{f(B)}-\frac{f(B)PV^*}{f(B^*)P^*V}-\frac{VP^*}{V^*P}\right)+c\theta\pi f(B^*)P^*\left(2-\frac{f(B^*)}{f(B)}-\frac{f(B)}{f(B^*)}\right).\end{aligned}$$

Finally, using the arithmetic-geometric means inequality, $n-(y_1+y_2+...+y_n)\leqslant 0$, where $y_1y_2...y_n=1$, and $y_1,y_2,...y_n>0$, it follows that $dL/dt\leqslant 0$. Furthermore, $dL/dt=0$ is equivalent to $(B,V,P)=(B^*,V^*,P^*)$. The global asymptotic stability of the EPE E^* follows from the classical stability theorem of Lyapunov and the LaSalle's Invariance Principle (see LaSalle J. P. (1976)). This result shows that, as long as $1<\mathscr{N}_0<\mathscr{N}_0^c$, the set Ω_{E^*} will never contain the periodic solutions.

5. Global sensitivity analysis of model's variables

We carry out sensitivity analysis to ascertain the uncertainty of the parameters to the model output. This is vital since it enables us to identify critical output parameters. Sensitivity and uncertainty analysis are performed using the Latin hypercube sampling (LHS) scheme, a Monte-Carlo stratified sampling method that allows to obtain an unbiased estimate of the model output for a given set of input parameter value. The parameter space is simultaneously sample is used to compute unbiased estimate of output values for state variables (see Ray C., Mariano S., Hogue I.B. & Kirschner D.E. (2008)). We use predefined variation of the model parameters at 10% and 50% relative to the referential values. Using algorithm from Ray C., Mariano S., Hogue I.B. & Kirschner D.E. (2008) , we compute the partial ranking correlation coefficient (PRCC) of parameters against model's variables B, V and P. We use a sample of size 1000 to identify relationship between parameters and output variables. A positive (negative) correlation coefficient corresponds to an increasing (decreasing) monotonic trend between the model's variable and the parameter under consideration. Note that a parameter is significantly correlate to one state variable if the absolute value of PRCC is greater than 0.5 and p-value less than 0.001.

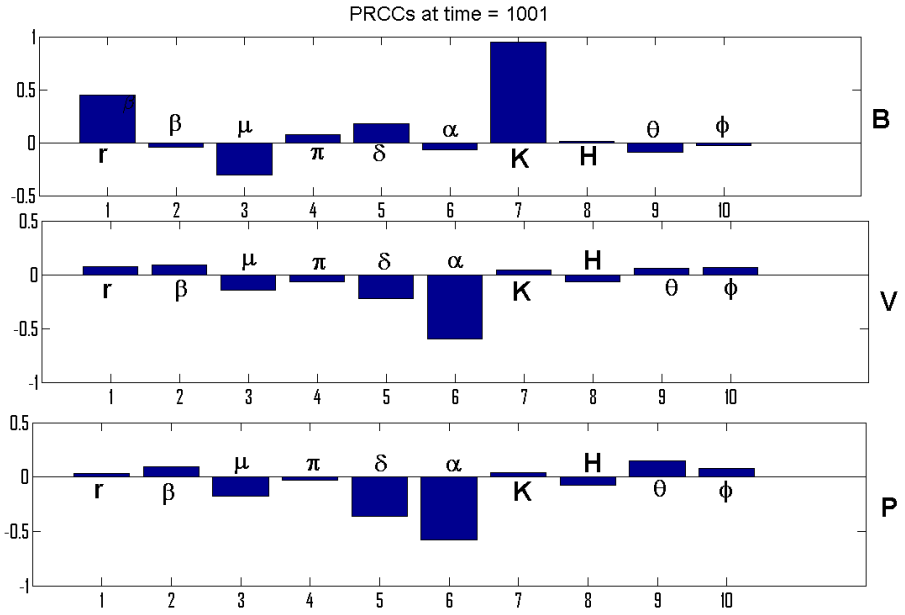

FIG. 9. Global sensitivity analysis (PRCCs) between B, V, P and each parameter.

REMARK 5.1 From Figure 3 and Figure 9, we can identify six parameters that strongly influence the population dynamics, namely: the contact rate (β), phage death rate (δ), bacteria carrying capacity (K), induction rate (α), burst size (θ) and cell division size (ϕ). We can then made the following suggestions:
(i) The use of more UV radiations and chemicals to increase the prophage induction could be an effective control measure against the growth of lysogen bacteria.
(ii) The use of biological control to reduce the bacteria cell division size.
(iii) The implementation of the methods proposed in Bhandare & Sudhakar G. (2005) in order to iden-

tify/select lytic phages and release them in the environment. This leads to the increase of contacts between bacteria and lytic phages which in turn favors the reduction of bacteria.

6. Conclusion

The objectives of this paper were fourfold:

(1) From the modeling perspective, we build a mathematical model for the phage-bacteria interactions in the environmental reservoir by taking into account the prophage induction process. This work considers three aspects of life cycles of phages and bacteria:

(a) The lytic life cycle: phages infect cells and the progeny phages are produced through lysis killing the bacteria and producing numerous phages.

(b) The lysogenic life cycle: phages do not kill cells and support the emergence of new clones of bacteria.

(c) The prophage induction event, that is the switching from lysogenic to lytic life cycle.

The resulted mathematical model obtained from these processes is a prey-predator like system with Holling type II functional response and logistic growth of free bacteria.

(2) From the theoretical analysis point of view, we do an in-depth investigation of asymptotic behavior and bifurcation analysis of the system. In this regard, we have computed the basic offspring number $\mathscr{N}_0$ and used it as the bifurcation parameter to establish the local/global stability of equilibria. Lyapunov-LaSalle techniques were used for the global asymptotical stability results and for the estimation of the basin of attraction of the locally asymptotically stable EPE. Based on the values and range of $\mathscr{N}_0$, all the equilibria were topologically classified using the center manifold approximation, and the types of bifurcation were specified accordingly. Precisely, we have shown that the system undergoes a trans-critical bifurcation around $\mathscr{N}_0 = 1$ and a Hopf bifurcation around the EPE.

(3) Computationally, we used MatLab platform to perform both the global sensitivity analysis of $\mathscr{N}_0$ and the model variables. The result of that sensitivity analysis suggests that, the contact rate β, the induction rate α, the bacteria carrying capacity K, the burst size θ and the cell division size ϕ are the more influential parameters on the phage-bacteria interactions. Moreover, we have simulated the system to illustrate our theoretical results: namely, the GAS of the PFE has been illustrated, as well as the occurrence of periodic solutions. Epidemiologically speaking, the existence of stable periodic solutions could explain the occurrence of repetitive outbreaks of some bacteria-borne diseases such as cholera in Africa and Asia.

(4) Finally, ecologically and epidemiologically speaking, we have provided the following responses to the two raised research questions in the introduction: For small values of the basic offspring number of phages, it is possible that periodic bacterial diseases outbreak occur. On the other hand, for sufficiently large values of the basic offspring number, the total population of bacteria go extinct and the polluted environment is purified.

Despite the high level of complexity of our work, it still offers many opportunities for extension. Since, it is well-documented that bacteriophages (and in particular vibriophages) can convert their bacterial hosts from non pathogenic strains to pathogenic strains through a process called phage conversion, by providing the hosts with phage-encoded virulence genes (for instance, toxigenic V. Cholerae isolates carry the ctxAB genes encoded by lysogenic phage), and that only those strains cause epidemic and pandemic cholera (see Faruque M. & John J. (2012)); our next work is to couple the model in this work with an epidemic cholera model in order to study the impacts of prophage induction and lysogen bacteria on the cholera dynamics. Furthermore, we intend later to include the innate immune system in our modeling framework to better investigate the perspective of phage therapy.

Acknowledgments

The fourth author (BT), acknowledges the support of the University of Pretoria Senior Postdoctoral Program Grant (2018-2020).

REFERENCES

ANDERSON R. & MAY R. (1991) *Infectious disease of human: Dynamics and control*, Oxford university press, Oxford, UK.

BHANDARE & SUDHAKAR G. (2005) *Biocontrol of V. cholerae using bacteriophages*. PhD thesis, University of Nottingham.

BERGE T., LUBUMA J.M.S., MOREMEDI G.M., MORRIS N.& KONDERA-SHAVA R. (2016) A simple mathematical model of Ebola in Africa, *J. Biol. Dyn.,* **11** (1), 42–74.

BERETTA E.& Y. KUANG (1998) Modelling and analysis of a marine bacteriophages infection, *Math. Biosci.,* **149**, 57–76.

BIRKHOFF.G& ROTA.G.C. (1989) *Ordinary Differential Equations*. New York.

CHAKRABORTY K., JANA S.& KAR T. K. (2012) Global dynamics and bifurcation in a stage structured prey-predator fishery model with harvesting, *Appl. Math. Comput.,* **218**,9271–9290.

CASTILLO.C& SONG.B., (2004) Dynamical models of tuberculosis and their applications, *Math. Biosci. Eng.,* **1** (2), 361–404.

CHAYU Y. & JIN M. (2018) On the intrinsic dynamics of bacteria in waterborne infection, *Math. Biosci.,* **296**, 71–81.

DAVIS B.M. & WALDO M.K. (2003) Filamentous phages linked to virulence of vibrio cholerae, *Curr. Opin. Microbiol.,* **6** (1), 35–42.

DRIESSCHE P.V.D. & WATHMOUGH J. (2002) Reproduction number and sub-threshold endemic equilibria for compartmental models of disease transmission, *Math. Biosci.* **180**, 29–48.

FAHAD B. & SANTANU R. & EZIO V. (2018) Role of media coverage and delay in controlling infectious diseases: A mathematical model, *Appl. Math. Comput.,* **337**, 372–385.

FARUQUE M. & JOHN J. (2012) Phage-bacterial interactions in the evolution of toxigenic vibrio cholerae, *Virulence*, **3** (7), 556–565.

FREMANN H., RUAN S. & TANG M. (1994) Uniform persistence and flows near a closed positively invariant set, *J. Diff. Equ.,* **6**, 583–600.

GUTTMAN B. & RAYA R.(2005) Bacteriophage: Biology and application, *CRC Press, USA,* 29–66.

GJORGJIEVA.J., SMITH K., CHOWELL G., SANCHEZ F., SNYDER D. & CASTILLO C. (2005) The role of vaccination in the control of SARS, *Math. Biosci. Eng.,* **2** (4), 21–17.

JENSEN A. FARUQUE M., & BRUCE R.(2006) Modeling the role of bacteriophage in the control of cholera outbreaks, *PNAS,***103**, 4652–4657.

JUDE D., WILLIAM D. & HAO W. (2014) Dynamics of a Cholera Transmission Model with Immunological Threshold and Natural Phage Control in Reservoir, *Bull. Math. Biol.,* **76**, 2025–2051.

LAKSHMIKANTHAM S. & LEELA M. (1989) *Stability analysis of non linear system,* Marcel Dekker, Inc, New York, Basel.

LASALLE J. P (1976) *The stability of Dynamical systems*, Brown University.

LASALLE J.P (1968) Stability theory for ordinary differential equations, *J. Differ. Equ.,* **4**, 57–65.

LUI F., CORTEZ M.& WEITZ J. (2013) Mechanism of multi-strain coexistence in host-phage system with nested infection network, J. *Theor. Biol.,* **332**, 68-77.

LIU W. M.(1994) Criterion of Hopf bifurcation without using eigenvalues, *J. Math. Anal. Appl.,* **182**, 150–162.

MILLER R. V.,& DAY M. (2008) Contribution of lysogeny, pseudo-lysogeny, and starvation to phage ecology, *Bacteriophage Ecology*, Cambridge university press, 114–143.

MISRA A.K., ALOK G. & EZIO V. (2016) Cholera dynamics with Bacteriophage infection: A mathematical study,*Chaos Sol. Frac.,* **91,** 610–621.

PAU G. & YING P. (2007) Global dynamics of a predator-prey model with stage structure for predator, *SIAM J. Appl. Math.,* **67** (5), 1379–1395

PRABIR P. & S HYAMAL K.M. (2005) Stability analysis of coexistence of three species prey-predator model, *J. Non. Dyn.,* **81**, 373–382.

PRABIR P. &SHYAMAL K.M (2017) Effect of toxicants on Pytoplankton-zooplankton-fish dynamics and harvesting, *Chaos. Sol. Frac.,* **104**, 389–399.

RAY C., MARIANO S., HOGUE I.B. & KIRSCHNER D.E.(2008) A methodology for performing global uncertainty and sensitivity analysis in system biology, *J. Theor. Biol.,* **254**, 178–096.

SHUIA Z. & DRIESSCHE P.V.D. (2013)Global stability of infectious disease models using Lyapunov functions, *J. Appl. Math.,* **73** (4) 1513–1532.

SUKHITA & VIDURUPOLA W. (2018) Analysis of deterministic and stochastic mathematical models with resistant bacteria and bacteria debris for bacteriophage dynamics,*Appl. Math. Comput.*, **316**, 215-228.

XIABONG T. & RUI X.(2011) Global dynamics of a predator-prey system with Holling type II functional response, *Nonlinear Anal. Model.,* **16** (2), 241–253.

XUEYING W. & JIN W. (2017) Modelling the within-host dynamics of cholera: Bacteria-viral interaction, *J. Biol. Dyn.,* **11**, 484–501.

YANG J. TANG S. & ROBERT A. (2013) Global stability and sliding bifurcation of a non-smooth Gause predator-prey system, *Appl. Math. Comput.,* **224**, 9–20.

YU P., NADEEM A. & WALL L. M. (2017) The impact of prophage on the equilibria and stability of phages and host, *J. Nonlinear. Sci.,* **27**, 817–846.